

# ELECTRONIC STRUCTURE AND MAGNETIC PROPERTIES OF IRON BY AB INITIO CALCULATIONS: RECENT ADVANCES

MOJMÍR ŠOB, MARTIN FRIÁK

Recent results of ab initio electronic structure calculations in iron are reviewed and their application to studies of magnetic properties, phase stability and extended defects is demonstrated. A special attention is paid to the bcc-hcp and bcc-fcc transformation paths and to the changes of magnetic ordering during those transformations. The role of ab initio calculations in atomistic modelling of extended defects such as grain boundaries, interphase interfaces, etc., is discussed.

**Key words:** electronic structure, magnetic moments, magnetic properties, first-principles electronic structure calculations

## ELEKTRONOVÁ STRUKTURA A MAGNETICKÉ VLASTNOSTI ŽELEZA Z PRVNÍCH PRINCIPŮ: AKTUÁLNÍ VÝSLEDKY

Článek podává přehled nejnovějších výsledků týkajících se elektronové struktury železa, které byly získány na základě výpočtů z prvních principů. Tyto výsledky jsou použity ke studiu magnetických vlastností, fázové stability a rozlehlých defektů. Zvláštní pozornost je věnována transformačním drahám bcc-hcp a bcc-fcc a změnám magnetického uspořádání během těchto transformací. Závěrem je diskutována úloha výpočtů elektronové struktury z prvních principů v atomistickém modelování rozlehlých defektů, jako jsou hranice zrn, mezifázové hranice atd.

### 1. Introduction

Most, if not all, of the properties of solids can be traced to the behavior of electrons, the "glue" that holds atoms together to form a solid. Thus, an important aim of the condensed matter theory is calculating of the electronic structure (ES) of solids. The theory of ES is not only helpful in understanding and interpreting

---

Doc. RNDr. Mojmír Šob, DrSc., Institute of Physics of Materials, Academy of Sciences of the Czech Republic, Žitkova 22, CZ-616 62 Brno, Czech Republic.

Mgr. Martin Friák, Faculty of Science, Masaryk University, Kotlářská 2, CZ-611 37 Brno, Czech Republic, and Institute of Physics of Materials, Academy of Sciences of the Czech Republic, Žitkova 22, CZ-616 62 Brno, Czech Republic.

experiments, but it also becomes a predictive tool of physics and chemistry of condensed matter and materials science.

To gain some basic understanding about the electronic structure and properties of materials, even very simple models based on empirical tight-binding approach which describe bonding in terms of the local environment of atoms may be used (for a review see e.g. [1, 2, 3]). These models involve a number of uncontrolled approximations, and while they give valuable insight and can even predict trends in properties, they contain parameters which must be fit either to experimental data or to the results of some more sophisticated calculations.

A lot of structural and dynamic properties of solids can be predicted accurately from first-principles (*ab initio*) calculations, i.e., from fundamental quantum theory (Schrödinger equation). Here the atomic numbers of the constituent atoms and, usually, some structural information are employed as the only pieces of empirical input data. Such calculations are routinely performed within the framework of density functional theory, in which the complicated many-body motion of all electrons is replaced by an equivalent but simpler problem of a single electron moving in an effective potential. The calculated total energies are used to obtain equilibrium lattice parameters, elastic moduli, relative stabilities of competing crystal structures for a given material, energies associated with point and planar defects, alloy heats of formation, etc. In addition to that, we also obtain information about electronic densities of states and charge densities, which enables us to get a deeper insight and learn which aspects of the problem are important.

During the last decade, or so, the ES theory exhibits a growing ability to understand and predict the material properties and to design new materials by computers. A new field of solid state physics and materials science emerged – computational materials science. It has achieved a considerable level of reliability concerning predictions of physical and chemical properties and phenomena, thanks in large part to a continued rapid development and availability of computing power (speed and memory), its increasing accessibility (via networks and workstations), and new computational methods and algorithms, which this permitted to generate. State-of-the-art ES calculations yield highly precise solutions of the one-electron Kohn-Sham equation for a solid and provide an understanding of matter at the atomic and electronic scale with an unprecedented level of detail and accuracy. In many cases, one is able not only to simulate experiment, but also to design new molecules and materials and to predict their properties before actually synthesizing them. A computational simulation can also provide data on the atomic scale that are inaccessible experimentally.

Until recently, most of the first-principles electronic structure calculations were performed in local density approximation (LDA) to the density functional theory. In this approximation, the many-body effects are included such that for a homogeneous electron gas the treatment is exact, and for an inhomogeneous system the

exchange and correlation are treated by assuming that the system is composed from many small systems with a locally constant density. Analogously, one may introduce the so-called local spin density approximation (LSDA) for spin-polarized systems.

The LDA and LSDA have been remarkably successful in describing the ground-state properties of a large range of physical problems. They proved to be surprisingly powerful both in a wide variety of cohesive properties and band structure calculations. This is the basis of their current acceptance and widespread utilization.

Despite its overall success, the LDA and LSDA have well documented deficiencies in quantitative total-energy calculations [4]. While ground-state properties (bond distances and angles, lattice constants etc.) are usually well estimated (within a few percent of their experimental values), L(S)DA are known to give a systematic overestimation of binding energies. (However, this problem is usually attributed to errors in the atomic reference calculations.)

## 2. First-principles electronic structure calculations in iron

Iron is located between antiferromagnetic and ferromagnetic regions in the Periodic Table. This location allows for a variety of magnetic structures. Thus, Fe exists in both bcc and fcc structures and has many magnetic phases, especially in thin films. The close competition between different magnetic states has also been confirmed by first-principles electronic structure calculations, as we discuss below.

In the case of Fe, the LSDA predicts a non-magnetic close-packed ground state instead of the ferromagnetic bcc phase found in nature [5, 6]. It turns out that inclusion of non-local effects through the generalized gradient approximation (GGA) overcomes this problem and stabilizes the bcc ferromagnetic state [6, 7]. This has also been verified in number of recent studies (see e.g. [8, 9, 10, 11]).

The state-of-the-art theoretical calculations based on GGA show unequivocally that magnetic order plays a most crucial role for the phase stability of iron and iron-based systems [12]. For example, the bcc  $\alpha$  phase of iron is stabilized by ferromagnetism at ambient conditions – neglecting magnetic order leads to a completely different order of structures, giving the hcp phase as most stable, even within the GGA (see e.g. [13, 9]). The analysis based on the Stoner model of ferromagnetism allows to locate other possible ferromagnetic solutions and contributes to a deeper understanding of magnetic behavior [14, 15, 16].

Magnetism is often responsible also for ordering in 3d-metal alloys. It was shown, for example, that if the magnetic moments in FeCo alloy are neglected, then the system would rather segregate than exhibit the ordered structure shown by experiment [17, 12]. The same type of magnetism-induced ordering was found also in the case of an FeCo overlayer on a Cu(001) substrate [17].

As it is discussed below, different magnetic states of iron are found also in the region of grain boundaries, ultrathin films, multilayers, etc. Recently, non-collinear spin-spiral states became a subject of both experimental and theoretical interest [18, 19]. Finite-temperature studies of magnetic effects from the first principles contribute to our understanding of the mechanisms of ferromagnetic-paramagnetic transition at the Curie temperature (see e.g. [20] and references therein).

All these findings indicate that for any realistic description of behavior of iron and iron-based systems, magnetic effects must be properly accounted for.

### 3. Properties and stability of higher-energy phases

Recently, investigations of energetics of higher-energy phases and of corresponding transformation paths attracted some attention [21, 22, 23]. It was found in a number of studies that atomic configurations in grain boundary regions or in thin films contain certain metastable structures, different from the ground-state structures. For example, the 9R ( $\alpha$ -Sm) structure was theoretically predicted and verified by high-resolution electron microscopy (HREM) at grain boundaries in silver and copper [24, 25]. Similarly, the bcc structure was found at certain grain boundaries in copper [26]. Occurrence of such phases at interfaces is even more likely in more complex non-cubic alloys such as TiAl. Indeed, new structural features of this alloy have been discovered very recently. Abe et al. [27] found a B19-type hcp-based structure in a Ti-48 at.%Al alloy quenched from the disordered phase, and Banerjee et al. [28] observed a series of structural transitions in the form of changes in the stacking sequence of the close-packed atomic planes in the Ti and Al layers in Ti/Al multilayered thin films.

Higher-energy structures appear also in thin films and precipitates. Ultrathin films of metastable fcc iron can be prepared epitaxially on fcc metal single-crystal surfaces up to thicknesses of a few monolayers. Pseudomorphic epitaxy on a (001) surface of a cubic metal usually results in a strained tetragonal structure of the film. In this case, there is a stress in the (001) plane keeping the structure of the film and of the substrate coherent, and the stress perpendicular to this plane vanishes. A tetragonal phase arises, which may be stable or metastable [29]. Typical example is face-centered tetragonal iron grown on the (001) Cu plane or in Fe/Cu multilayers ([30] and the references therein). Similarly, an epitaxial film grown on the (111) plane of a cubic substrate may exhibit a trigonal deformation of its lattice. Magnetic properties of fcc or face-centered tetragonal iron are very sensitive to atomic spacing imposed by the substrate or by the matrix [31]. For example, small fcc particles may be antiferromagnetic in Cu whereas they may be ferromagnetic in Cu-Au alloys in which they have a larger lattice spacing. Similarly, while on Cu(001) both a high-spin tetragonally distorted phase and a low-spin fcc phase have been reported [32], the thermally deposited iron films on Cu(111) exhibit low-spin ferromagnetic or ferrimagnetic phases [33]. Ohresser et al. [34] reported

different structural and magnetic behavior of ultrathin iron films grown by pulsed-laser deposition on Cu(111) surface from those obtained by thermal deposition: the pulsed-laser deposition results in an improvement of the quality of the film structure and leads also to a delay of the fcc to bcc phase transformation whose critical thickness (6 monolayers) is twice as large as that of thermally deposited films.

Technologically, the bcc to fcc and martensitic transformations are very important as they constitute a basis of steel-making industry. Although the mechanisms of these transformations have been studied for a long time, they are still not fully understood [35]. From the geological point of view, high-pressure phases of iron are very exciting as iron is the dominant component of the Earth's core. Ferromagnetic bcc iron undergoes a phase transition to non-spin-polarized hcp phase at 13 GPa. First-principles studies of behavior of iron up to earth-core pressures have already been performed [8, 36]. Recently, a new phase at high pressure ( $> 30$  GPa) and high temperature ( $> 1800$  K) has been discovered, however, there is a controversy if its structure is orthorhombic or dhcp [37].

To explore adequately thin films, extended defects and phase transformations, a detailed information about energetics of possible metastable structures as well as lattice transformations connecting them is needed. Armed with this knowledge one can predict, for example, whether an interface may be associated with a metastable structure and assess thus its stability and ability to transform to other structures (for example during deformation or due to changes in stoichiometry).

Craievich et al. [22] have shown that some energy extrema on constant-volume transformation paths are dictated by the symmetry. Namely, most of the structures encountered along the transformation paths between some higher-symmetry structures, say between bcc and fcc (Bain's path) or between bcc and hcp, have a symmetry that is lower than cubic or hexagonal. At those points of the transformation path where the symmetry of the structure is higher the derivative of the total energy with respect to the parameter describing the path must be zero (for example, at those points of the Bain's path where the structure is bcc or fcc). These are the so-called symmetry-dictated extrema. However, other extrema may occur that are not dictated by symmetry and reflect properties of the specific material. Configurations corresponding to energy minima at the transformation paths represent stable or metastable structures and may mimic atomic arrangements that could be encountered when investigating extended defects such as interfaces and dislocations [23, 38].

In this paper, we would like to illustrate the applications of first-principles calculations to bcc-hcp and bcc-fcc transformations in iron. During those transformations, iron changes its spin-polarized (ferromagnetic) state to a non-spin-polarized one (bcc-hcp transformation) or to a spin-polarized state with a lower magnetic moment (bcc-fcc transition). Both transformations are, in fact, magnetic first-

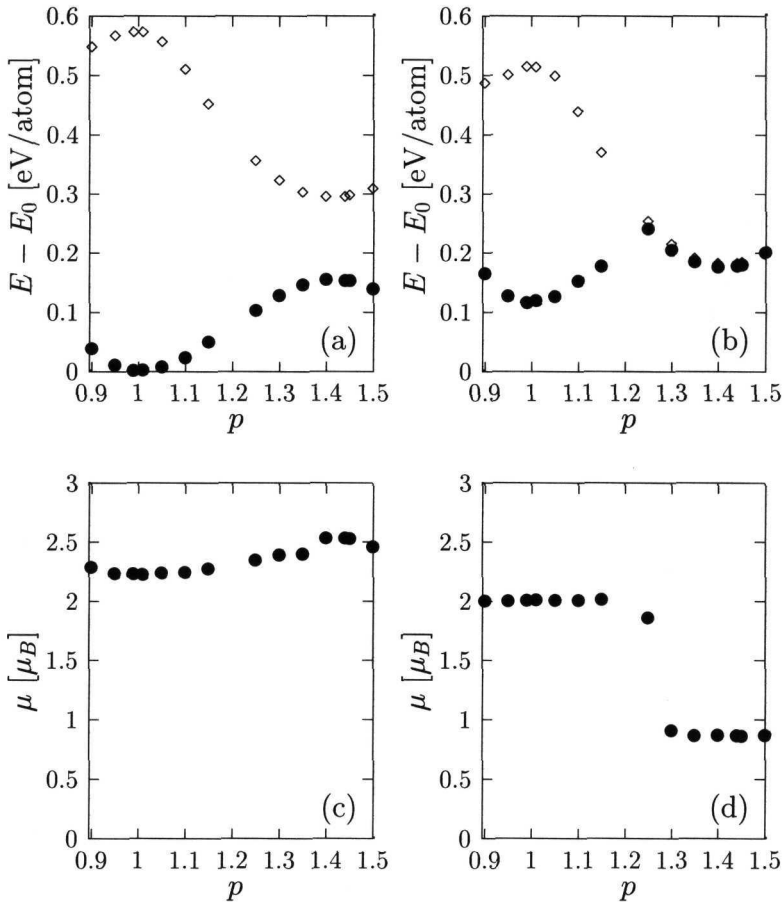


Fig. 2. Variations of total energies and magnetic moments along the constant-volume bcc-fcc (Bain's) transformation path. Here,  $E_0$  is the ground state energy of bcc FM iron and  $p = c/a$  is the parameter of the path. Full circles represent results of FM calculations and diamonds of NM calculations. Figures (a) and (c) correspond to the experimental lattice volume per atom ( $a_{\text{bcc}} = 5.408$  au), figures (b) and (d) to the equilibrium volume of the hcp structure (the lattice parameter of the bcc lattice with the same volume per atom is  $a_{\text{bcc}} = 5.1644$  au). In the right-hand side of figure (b), the energies of the FM states are only very slightly lower than the energies of the NM states.

(up to  $p = \sqrt{2}$ ) could be generated [51]. Up to  $a_{\text{bcc}} = 5.395$  au, the FM states in the vicinity of  $p = \sqrt{2}$  possess higher energies than the corresponding NM states and are, therefore, unstable.

Fig. 2 shows the same results for the bcc-fcc transformation path which is the

usual Bain's path connecting the bcc and fcc structures via tetragonal deformation. At constant volume, the deformed structures can be parametrized in terms of the  $c/a$  ratio, which will be henceforth also denoted by the symbol  $p$ . If we ascribe the value  $p = 1$  to the bcc structure, then the fcc structure is obtained for  $p = \sqrt{2}$ .

It may be seen that the energy difference between the NM and FM fcc structures at experimental (bcc FM) atomic volume is higher than the difference between the NM and FM hcp structures (cf. Figs. 1a and 2a). However, a qualitative change is encountered at the equilibrium volume of the NM hcp structure (cf. Figs. 1b and 2b, 1d and 2d). At  $p \approx 1.25$ , we may see a transition from the high-spin FM state with the magnetic moment of about  $2.0 \mu_B$  to a low-spin FM state with the magnetic moment of about  $0.9 \mu_B$ . The magnetic moments in both high-spin and low-spin region are nearly independent of the parameter of the path,  $p$ . Our finding correlates very well with the results of Körling and Ergon [18] who found a low-spin FM state for fcc iron ( $p = \sqrt{2}$  in Fig. 2) for volumes equivalent to  $a_{\text{fcc}} \lesssim 6.75$  au, i.e.  $a_{\text{bcc}} \lesssim 5.36$  au. Paper [18] indicates that the energy of the antiferromagnetic (AF) states may be lower than that of the FM states for the fcc structure and its neighborhood. Therefore, analysis of the behavior of the AF state along the tetragonal transformation path is highly desirable [51].

From the point of view of the bcc-hcp transformation, the transition region between the NM and FM states (the region of crossing of the FM and NM curves) and the dependence of the energy at these crossing points on volume is most interesting. This is the topic of a subsequent publication [51].

We were also able to reproduce the trends of the behavior of the bcc lattice constant at the early stages of the bcc-hcp experiment performed recently by Wang and Ingalls [52]. Fig. 3 shows our theoretical values in comparison with experiment. Wang and Ingalls observed a strong increase of the bcc lattice constant  $a_{\text{bcc}}$  at increasing pressure between 14 and 19 GPa, a plateau corresponding to a relatively large value of  $a_{\text{bcc}}$  upon release of pressure, and strong decrease of  $a_{\text{bcc}}$  at decreasing pressure between 12 and 10 GPa. Of course, we were not able to describe this hysteresis behavior on the basis of our calculations, as it is probably caused by the interfacial strains between the two phases which we could not include. However, the decreasing part of the  $a_{\text{bcc}}$  as a function of pressure is reproduced quite well. A small shift of the theoretical and experimental values ( $\approx 0.5\%$ ) may be partly due to approximations involved in the GGA and by the fact that the measurements were performed at the room temperature, but the calculated results correspond to 0 K. Let us note that the slope of the curves in Fig. 3 at zero pressure is proportional to the bulk modulus.

Wang and Ingalls [52] gave a very plausible explanation of the observed hysteresis behavior in terms of interfacial strains. However, it might be also influenced by magnetic effects. In the two-phase regime, there are spin-polarized (ferromagnetic) and non-spin-polarized regions. It is not excluded that the changes in the

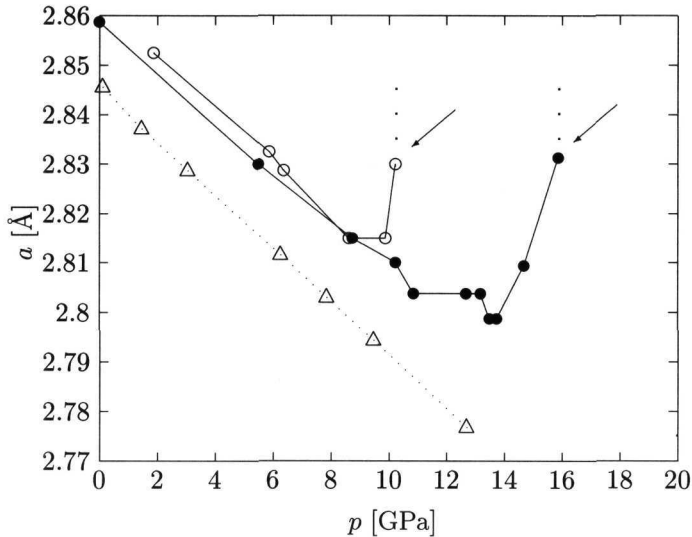


Fig. 3. Lattice constant of the bcc phase  $a_{\text{bcc}}$  as a function of pressure. Filled (open) circles represent the experimental results of Wang and Ingalls [52] at increasing (decreasing) pressure; the arrows show the beginning of the hysteresis loop. Our theoretical results are represented by triangles.

magnetostatic energy during the transformation could influence the energetics of the process.

#### 4. First-principles calculations of extended defects in iron

Many of the material properties are determined to a large extent by the properties of defects such as vacancies, dislocations, grain, antiphase and interphase boundaries, etc. The study of the behavior of polycrystalline materials is often reduced to the study of the behavior of their internal interfaces.

Grain boundaries are regions of transition between two identical but mutually rotated adjacent single crystal pieces. They are different from the bulk in their atomic structure and very often also in composition if, for example, segregation of impurities at grain boundaries takes place. They affect strongly physical and mechanical properties of material. Grain-boundary cohesion is one of the determining factors of mechanical strength and of the resistivity against intergranular fracture.

Despite the considerable effort invested into the study of magnetic surfaces, overlayers and epitaxial interfaces (see e.g. [53]), comparatively little is known about the magnetic and electronic properties of grain boundaries in magnetic materials. On the basis of the finely tuned interplay between magnetism and structure

in iron, we may expect a variety of structure-magnetism-property relations. Here, first-principles calculations may yield valuable information as the processes connected with the change of the magnetic state are determined by the changes in the underlying electronic structure.

The most studied grain boundary in iron is  $\Sigma = 3(111)$ . Gonis et al. [54] found a significantly enhanced magnetic moment at the boundary above the bulk value. Similar conclusion was arrived at for the  $\Sigma = 5(310)$  tilt grain boundary [55, 56, 57]. No lattice relaxation was performed in these studies.

Most studies of the  $\Sigma = 3(111)$  grain boundary were devoted to the effect of segregated impurities (H, B, C, P, S, Mn) on grain boundary cohesion ([58, 59] and references therein). It was shown that B and C are “cohesion enhancers” whereas the other metalloid impurities diminish the grain boundary cohesion. In [59] it was confirmed that Mn atoms facilitate embrittlement in the grain boundary due to P impurities. Sizeable structure relaxations were found in Mn+P decorated grain boundaries, connected with closely related changes in electronic and magnetic properties. The role of B as a “cohesion enhancer” was confirmed also at the  $\Sigma = 5[100]$  grain boundary [60].

Number of atoms relaxed in the above studies was not very large ( $< 100$ ) and, in addition to that, often only vertical interplanar distances were adjusted on the basis of calculated interatomic forces [59]. To include more degrees of freedom to perform full relaxation within a sufficiently large region around the grain boundary, we have to resort to simpler schemes as, e.g., tight-binding or bond-order potentials approach where the effect of magnetism is properly included [40, 41, 42, 43, 44]. The treatments like embedded atom method [45] or Finnis-Sinclair central-force potentials [46] cannot be used in cases where the magnetic effects are essential as there is, at present, no way to include them.

## 5. Conclusions

The significance of first-principles calculations consists in the high reliability of predictions of new properties and phenomena. There are no adjustable parameters and well defined approximations are introduced on the most fundamental level. Nevertheless, similarly as in other atomistic studies, the goal of the electronic structure calculations is not to obtain numbers, but insights. The results include electronic wavefunctions, charge densities and magnetic moments. On the basis of these results, further material characteristics may be calculated, e.g. cohesive energy, elastic constants, some strength characteristics, magnetic susceptibility, transport coefficients, etc., and some aspects of the phase transformations may be described. Specifically, in this paper we have shown how the first-principles electronic structure calculations may contribute to a deeper understanding of some aspects of bcc-hcp and bcc-fcc phase transformation. Similarly, they also show that the magnetic moment is significantly different at grain boundaries when compared

with the bulk [56, 57]. This phenomenon was not considered in previous studies of atomic structure and properties of interfaces, although it may substantially affect the interfacial cohesion and other characteristic quantities [41]. The information available from the first-principles calculations allow us both to test and construct simpler models (tight-binding, bond-order potentials, Finnis-Sinclair central-force potentials, embedded atom model), which, in turn, may be used in very extensive atomic level studies while the state-of-the-art first-principles calculations can only be made for a relatively small number of atoms (less than  $\approx 100$ ).

The first-principles calculations may also be used for "measurements in the computer". Thus, computer simulations can substitute a real experiment and, more importantly, provide data on atomic scale that are not accessible experimentally. We expect that in future the first-principles methods will contribute most significantly to studies of electronic structure and atomic configuration of extended defects, especially in systems with covalent bonds, such as non-close-packed metals, non-cubic intermetallics, metal-ceramic interfaces, semiconductor systems, etc.

Notwithstanding, simpler methods, such as embedded atom method [45] and N-body central force potentials [46], will remain essential for studies of very large non-magnetic systems. However, it is imperative to combine simpler methods with the first-principles approaches on one side and experiment on the other one.

### Acknowledgements

This research was supported by the Grant Agency of the Academy of Sciences of the Czech Republic (Project No. A1010817) and by the Grant Agency of the Czech Republic (Project No. 106/99/1178). The use of computer facilities at the MetaCenter of the Masaryk University, Brno, within the grants FRVS F0631/96 and MŠMT 98272 is acknowledged.

### REFERENCES

- [1] HARRISON, W. A.: *Electronic Structure and the Properties of Solids*. New York, Dover Publications 1989.
- [2] SUTTON, A.: *Electronic Structure of Materials*. Oxford-New York, Clarendon Press 1993.
- [3] PETTIFOR, D. G.: *Bonding and Structure of Molecules and Solids*. Oxford-New York, Clarendon Press 1995.
- [4] JONES, R. O.—GUNNARSSON, O.: *Rev. Mod. Phys.*, **61**, 1989, p. 689.
- [5] WANG, C. S.—KLEIN, B. M.—KRAKAUER, H.: *Phys. Rev. Lett.*, **54**, 1985, p. 1852.
- [6] SINGH, D. J.—PICKETT, W. E.—KRAKAUER, H.: *Phys. Rev. B*, **43**, 1991, p. 11628.
- [7] BAGNO, P.—JEPSEN, O.—GUNNARSSON, O.: *Phys. Rev. B*, **40**, 1989, p. 1997.
- [8] STIXRUDE, L.—COHEN, R. E.—SINGH, D. J.: *Phys. Rev. B*, **50**, 1994, p. 6442.
- [9] MORONI, E. G.—KRESSE, G.—HAFNER, J.: *Phys. Rev. B*, **56**, 1997, p. 15629.
- [10] ELSÄSSER, C.—ZHU, J.—LOUIE, S. G.—FÄHNLE, M.—CHAN, C. T.: *J. Phys.: Condens. Matter*, **10**, 1998, p. 5081.

- [11] ELSÄSSER, C.—ZHU, J.—LOUIE, S. G.—MEYER, B.—FÄHNLE, M.—CHAN, C. T.: *J. Phys.: Condens. Matter*, 10, 1998, p. 5113.
- [12] ABRIKOSOV, I. A.—JAMES, P.—ERIKSSON, O.—SÖDERLIND, P.—RUBAN, A. V.—SKRIVER, H. L.—JOHANSSON, B.: *Phys. Rev. B*, 54, 1996, p. 3380.
- [13] ASADA, T.—TERAKURA, K.: *Phys. Rev. B*, 46, 1992, p. 13599.
- [14] KRASKO, G. L.: *Phys. Rev. B*, 36, 1987, p. 8565.
- [15] MARCUS, P. M.—MORUZZI, V. L.: *Phys. Rev. B*, 38, 1988, p. 6949.
- [16] KRASKO, G. L.—OLSON, G. B.: *Phys. Rev. B*, 40, 1989, p. 11536.
- [17] KUDRNOVSKÝ, J.—TUREK, I.—PASTUREL, A.—TETOT, R.—DRCHAL, V.—WEINBERGER, P.: *Phys. Rev. B*, 50, 1994, p. 9603.
- [18] KÖRLING, M.—ERGON, J.: *Phys. Rev. B*, 54, 1996, p. 8293.
- [19] LORENTZ, R.—HAFNER, J.: *Phys. Rev. B*, 58, 1998, p. 5197.
- [20] ROSENGAARD, N. M.—JOHANSSON, B.: *Phys. Rev. B*, 55, 1997, p. 14975.
- [21] MARCUS, P. M.—MORUZZI, V. L.: *J. Appl. Phys.*, 63, 1988, p. 4045.
- [22] CRAIEVICH, P. J.—WEINERT, M.—SANCHEZ, J. M.—WATSON, R. E.: *Phys. Rev. Lett.*, 72, 1994, p. 3076.
- [23] ŠOB, M.—WANG, L. G.—VITEK, V.: *Comput. Mat. Sci.*, 8, 1997, p. 100.
- [24] ERNST, F.—FINNIS, M. W.—HOFMANN, D.—MUSCHIK, T.—SCHÖNBERGER, U.—WOLF, U.: *Phys. Rev. Lett.*, 69, 1992, p. 620.
- [25] HOFMANN, D.—FINNIS, M. W.: *Acta Metall. Mater.*, 42, 1994, p. 3555.
- [26] SCHMIDT, C.—ERNST, F.—FINNIS, M. W.—VITEK, V.: *Phys. Rev. Lett.*, 75, 1995, p. 2160.
- [27] ABE, E.—KUMAGAI, T.—NAKAMURA, M.: *Intermetallics*, 4, 1996, p. 327.
- [28] BANERJEE, R.—AHUJA, R.—FRASER, H. L.: *Phys. Rev. Lett.*, 76, 1996, p. 3778.
- [29] ALIPPI, P.—MARCUS, P. M.—SCHEFFLER, M.: *Phys. Rev. Lett.*, 78, 1997, p. 3892.
- [30] LLOYD, S. J.—DUNIN-BORKOWSKI, R. E.: *Phys. Rev. B*, 59, 1999, p. 2352.
- [31] MORUZZI, V. L.—MARCUS, P. M.—KÜBLER, J.: *Phys. Rev. B*, 39, 1989, p. 6957.
- [32] ZHARNIKOV, M.—DITTSCHAR, A.—KUCH, W.—SCHNEIDER, C. M.—KIRSCHNER, J.: *J. Magn. Magn. Mater.*, 174, 1997, p. 40.
- [33] SHEN, J.—KLAUA, M.—OHRESSER, P.—JENNICHES, H.—BARTHEL, J.—MOHAN, CH. V.—KIRSCHNER, J.: *Phys. Rev. B*, 56, 1997, p. 11134.
- [34] OHRESSER, P.—SHEN, J.—BARTHEL, J.—ZHENG, M.—MOHAN, CH. V.—KLAUA, M.—KIRSCHNER, J.: *Phys. Rev. B*, 59, 1999, p. 3696.
- [35] ROITBURD, A. L.: *Mat. Sci. Eng. A*, 127, 1990, p. 229.
- [36] SÖDERLIND, P.—MORIARTY, J. A.—WILLS, J. M.: *Phys. Rev. B*, 53, 1996, p. 14063.
- [37] DUBROVINSKY, L.—SAXENA, S. K.—LAZOR, P.—WEBER, H. P.: *Science*, 281, 1998, p. 11a; ANDRAULT, D.—FIQUET, G.—KUNZ, M.—VISOCEKAS, F.—HAÜSERMAN, D.: *Science*, 281, 1998, p. 11a.
- [38] PAIDAR, V.—WANG, L. G.—ŠOB, M.—VITEK, V.: *Modelling and Simulation in Mat. Sci. Eng.*, 7, 1999, p. 369.
- [39] EKMAN, M.—SADIGH, B.—EINARSDOTTER, K.—BLAHA, P.: *Phys. Rev. B*, 58, 1998, p. 5296.
- [40] ZHONG, W.—OVERNEY, G.—TOMÁNEK, D.: *Phys. Rev. B*, 47, 1993, p. 95.
- [41] YEŞİLLETEN, D.—NASTAR, M.—ARIAS, T. A.—PAXTON, A. T.—YIP, S.: *Phys. Rev. Lett.*, 81, 1998, p. 2998.

